UDC 551.515.23:551.509.327(6) 551.507.362.2(084.12)

# SYNOPTIC HISTORIES OF THREE AFRICAN DISTURBANCES THAT DEVELOPED INTO ATLANTIC HURRICANES

TOBY N. CARLSON

National Hurricane Research Laboratory, ESSA, Miami, Fla.

ABSTRACT

Surface and upper air (700 mb) analyses along with high-quality satellite photographs are presented for a 2-week period during August and September 1967. These show, in particular, the structure and motion over the continent of Africa of four major wave disturbances, three of which later became Atlantic hurricanes. The evolution of cloudiness and convection and the intensification of the disturbance at low levels over West Africa are examined in detail and related to certain climatological features of the area. Some general characteristics of the disturbances are discussed.

## 1. INTRODUCTION

In a recent article by Simpson et al. (1968) summarizing the origin and movement of Atlantic tropical disturbances during the 1967 hurricane season, it was pointed out that about one-half of the 61 disturbances tracked by satellite photographs and ship reports across the tropical Atlantic were first observed close to the African Continent. About one-half of these were classed as tropical depressions, almost all of which formed during August and September. Of the 25 disturbances in the Caribbean that were not associated with a cold Low, 12 were traceable back to the African coast. Out of a seasonal total of six hurricanes and two tropical storms, three hurricanes and both tropical storms developed from African disturbances.

Similar statistics probably apply to other seasons as well as that of 1967, but there have been only a few well-documented cases of hurricanes forming from African disturbances. Such documentary evidence (e.g., the formation of hurricanes Debbie, 1961 (Erickson, 1963), and Anna of that same year (Arnold, 1966)) has shown that the hurricane formed from an African system that had been a particularly well-developed wave perturbation in the upper easterly flow over the continent prior to its arrival at the coast of Africa. Less explicit examples of such development are to be found in annual summaries of hurricane activity (Dunn, 1961; Dunn and Staff, 1962, 1963, 1965; Sugg, 1966, 1967) that describe the destructive hurricane Donna of 1960, hurricane Becky of 1962, hurricanes Florence and Gladys of 1964, hurricanes Betsy and Carol of 1965, and hurricanes Faith and Inez of 1966 as having originated near the African coast. Undoubtedly, had better satellite data been available for those years and more effort expended, other hurricanes and tropical storms would have been tracked back to this region.

An excellent opportunity for studying the nature and possible origin of disturbances over Africa prior to their intensification into the hurricane stage presented itself during the 1967 hurricane season when, following the advent of the high quality satellite pictures from ESSA 5, hurricanes Arlene, Beulah, and Chloe originated from disturbances that crossed the West African coast in the incipient stage during a 10-day period from August 24 to September 3. It is the purpose of this paper to present in some detail a synoptic account of these disturbances as they moved across the Continent of Africa. Satellite, surface, and upper air data are combined to serve as a guide for early recognition of incipient hurricanes over West Africa.

## 2. ANALYSIS

In order to describe the important features of the weather associated with traveling disturbances, the 1200 GMT streamlines at 2,000 and 10,000 ft (700 mb) and the surface pressures were analyzed for each of 15 successive days from August 21 to September 5. The area of analysis over land was prescribed by the data network, which is interrupted at the Sudanese border in the east and at the desert in the north. The western edge of the analysis is terminated at the Cape Verde Islands. Although figure 1 suggests that the coverage of surface and upper air data in the area is abundant, the actual transmission of reports from stations was erratic. Many stations, in fact, transmitted at different times on different days and sometimes not at all. Other stations reported occasionally or transmitted at 0600 or 1800 GMT. Since the diurnal fluctuations were often larger than those produced by weather systems and since many stations contained an appreciable bias in the surface pressure as the result of a barometric inconsistency, a procedure was followed for all stations to maximize the quality and density of data. This procedure was to examine in linear display the 15-day records and recover the missing pressure data, where possible, from the 24-hr pressure change values that are transmitted for all sub-Sahara stations. Next, the average pressures were computed at 1200 GMT, and a mean isobaric map (fig. 1) constructed. The magnitude of adjustment necessary to make the station pressure fit the analysis was considered as a constant bias to be added to the individual values. A similar procedure was used to obtain the diurnal corrections, from which further estimates of 1200 GMT pressure were made, using an interpolation of off-time reports and their 24-hr pressure tendencies.

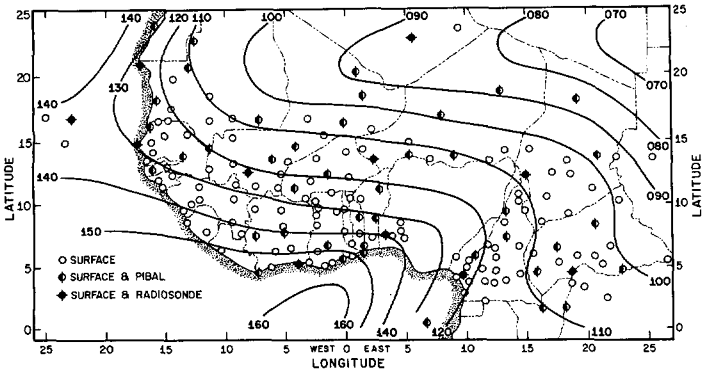


FIGURE 1.—Mean sea-level isobars at 1200 GMT for the period Aug. 21–Sept. 4, 1967. Contours are labeled in millibars and tenths above 1000. The distribution and type of reporting stations are indicated by the circles.

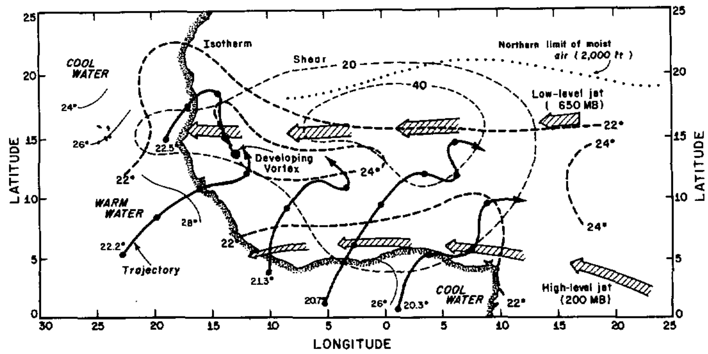


FIGURE 2.—Lower tropospheric zonal vertical shear (light dashed lines labeled in knots), wet-bulb potential temperature at 950 mb (heavy dashed lines labeled in °C), and air trajectories at 2,000 ft for 1200 GMT, Sept. 3, 1967. The 950-mb wet-bulb potential temperature at the origin of the trajectory is indicated by a single figure. Duration of travel in days is equal to the number of segmented intervals along the trajectory. Sea-surface temperatures (thin lines labeled in °C) were taken from values obtained by the research vessel *Geronima* during early August 1963. Representative positions of the low- and high-level easterly jet streams are indicated. The center of a developing surface depression is shown by a filled circle.

Wind reports were also erratic during this period. In some instances interpolation between off-time soundings was used to construct the 1200 GMT streamline maps, but in general the data were plotted at the station location as if they applied to 1200 GMT. When it became apparent that the weather systems were translatory, the first analyses were used to construct a second set of maps in which off-time data were displaced longitudinally from the station circle by a distance equal to the appropriate wave speed times the time differential from 1200 GMT (6 or 12 hr). In addition, surface wind and ship reports were used in places to supplement the 2,000-ft winds.

Besides the surface and upper air analyses, satellite pictures, such as those shown by Simpson et al. (1968), furnished a highly visual aid in identifying and following the weather systems. Because the satellite scans coincide with local noon, the photographs, digitally rectified to map coordinates, were highly relevant to the 1200 GMT analyses and are presented next to them.

## 3. CLIMATOLOGICAL BACKGROUND

It has been known for some time that wavelike disturbances in the easterly flow, associated with squally weather at the surface, move westward across the bulge of West Africa during the monsoon season of June–October (see Arnold, 1966, for example). During the early part of the season their occurrence is sporadic and they tend to be rather weak, but by August, when the depth and northward penetration of the moist southwesterly monsoon air are the greatest, the disturbances are rather more intense and are observed to pass Dakar at intervals of 3 or 4 days. Even in these months there may be periods of relative inactivity lasting from several days to a week or two. Both Erickson and Arnold found that the perturbations originated somewhere east of longitude 10°–20°E and moved westward at a fairly regular speed of about 15 kt. The accompanying cloudiness and bands of thunderstorms are undoubtedly related to Eldridge's (1957) traveling disturbance lines, which consist of more-or-less north-south-oriented line squalls. These are known to produce quite violent weather over the interior, but are somewhat less intense as they reach the western coastline.

The flow pattern over West Africa is strongly dominated by the effect of the Sahara Desert, a vast area of uniformly high potential temperature ($\theta \sim 45$°C) and low relative humidity throughout much of a very deep layer of dry convection. In contrast, the Atlantic Ocean and Gulf of Guinea comprise a relatively cold area ($\theta \sim 25$°C) over which a shallow southwesterly current of moist air flows inland, cutting across the isobars from a subequatorial high-pressure cell (see figs. 1 and 2). Interestingly, both the extremes of cold sea-surface temperatures in the Gulf of Guinea and warmth over the Sahara Desert are reached in August. Between the relatively cold waters of the Gulf of Guinea and the cold North Equatorial Current flowing southward along the African coast exists a narrow tongue of warmer water, associated with an equatorial countercurrent, which is warmest in late August.

The thermal wind produced by this striking temperature gradient results in a very rapid increase in easterly wind with height over the land and the existence of a strong easterly current aloft (see Reiter, 1963). During the late summer months the transition level between the easterly and westerly flow slopes upward from its intersection with the surface at about 20° lat. to a height of about 1 or 2 km at 5°–10°N, south of which the transition ceases to become well defined and the winds themselves are light. At middle levels the temperature gradient reverses from that at low levels, and the thermal wind reversal leads to a very narrow easterly jet, centered between 600 and 700 mb and at 15°–17°N. The strength of this jet is variable in time and space and is often as high as 30 or 40 kt (a shear of 40 or 50 kt from 2,000 ft). Outside the region of the African bulge the meridional temperature contrast is less pronounced, and the strong middle-level easterlies are therefore confined to the area between long. 15°E and 20°W (see fig. 2).

The velocity of the disturbances is about equal to that of the mean tropospheric wind and is contrary in direction to the low-level flow. The basic easterly current overlying the moist monsoon current enables the convective disturbances to possess the characteristic, unique for Africa, of long-term propagation. The strong wind shear and lid of drier air aloft somewhat resemble conditions found over the Middle West of the United States and may be responsible for producing a similarly violent convection.

West of longitude 15°E and south of about lat. 8°–10°N, the uncommon occurrence of intense thunderstorms during the months of August and September, traveling or otherwise, is due not so much to the absence of any strong basic current but to a notable lack of convective instability at low levels in air whose recent origin had been over the cold Gulf of Guinea. According to figure 2, the wet-bulb potential temperature, $\theta_w$, at 950 mb (the cloud base), as estimated from surface conditions using appropriate lapse rates of temperature and dewpoint, is closely related to the sea-surface temperature in the region where the 2,000-ft trajectories show the air to be originating. Temperature soundings for West Africa show that a parcel of air lifted from 950 mb is convectively unstable throughout most of the troposphere when its $\theta_w$ exceeds about 22.5°C. Air originating over the Gulf of Guinea is therefore stable as it crosses the southern coast of West Africa but it later achieves a marginal instability north of about 10° lat. Air originating over the warm current of water south of the Cape Verde Islands is initially somewhat unstable, having a $\theta_w$ at cloud base of about 22.5°, and later achieves a rather large instability over a wide portion of the interior. Disturbances that pass through this region of high instability can be expected to intensify, although the convection itself will once more become weaker along the immediate coast and out over the ocean. Of course, other factors, such as large-scale descent in this area, can cause the disturbances to dampen once they reach the coast.

Before proceeding to the individual wave disturbances, some remarks concerning the interpretation of the satellite photographs may be useful.

From an analysis of the cloud data, available from the standard synoptic reports, it was found that five or six characteristic weather types could be readily identified by their brightness and texture on the satellite pictures. The following descriptions are pertinent only to the vicinity of sub-Sahara West Africa during August and September:

A) *Intense convection:* thunderstorms associated with cumulonimbus clouds and accompanied by heavy precipitation. Appears on digitalized satellite photographs as a white, bright area. An example of this type is shown for August 22 (fig. 5d).

B) *Weak convection:* heavy, dense middle and high cloud with some showers. Low clouds either suppressed or with some swelling cumulus. Appears on satellite pictures as a smooth, light gray area surrounding convective regime (fig. 5d).

C) *Stratiform:* much of the cloud seen over tropical West Africa, south of 10°N, falls into this category. Low cloud is broken-to-overcast stratocumulus or stratus having little or no precipitation. Middle and high cloud cover, when visible at the surface, is broken to overcast. It appears on satellite pictures as a mottled and lusterless gray (fig. 5d).

D) *Rain, not associated with thunderstorms:* light or moderate precipitation; intermittent and showery and usually associated with stratiform variety of cloud cover. This type appears smoother and thicker than stratiform (fig. 5d).

E) *Broken stratiform:* similar to stratiform type but lower clouds are broken and may consist of cumuliform as well as stratiform cloud. Middle and high cloud cover tends to be highly broken. It appears on satellite pictures as a mottled gray with numerous open spaces (fig. 5d).

F) *Fair weather:* few or scattered low clouds, usually cumulus. Middle and high cloud cover is thin and up to broken cover. It appears on satellite pictures as a mostly open area with faint gray streaks (fig. 5d).

## 4. THE WAVE DISTURBANCES

During the 15-day period a total of six wave disturbances reached the west coast of Africa; a seventh already existed over the ocean on the 21st. Two of the six waves were weak and short lived, leaving four waves of similar intensity and character, each of which accompanied the formation of a major depression at surface near the coast of West Africa (fig. 3). For discussion purposes the *mean* longitude of wave axis (wind shift line) at 700 mb, which was adjusted for continuity of motion to remove sudden jumps in speed, is designated by an arrow and labeled according to a system followed by Arnold (1966). This discussion is concerned primarily with the four major disturbances, W–1, W–3, W–4, and W–6. It should be pointed out that because of the rather large (for low latitudes) pressure gradient across the lower portion of West Africa the existence of a vortex center may not be significant in itself insofar as a greater amount of vorticity may be concentrated in the high-speed portion of the wave. Similarly, an apparently closed isobar at sea level may not be present, despite obvious pressure falls there.

Wave W–1 (later to become hurricane Arlene) appears on the 21st with its axis near long. 5°E (see the sequence of figs. 4–9). During the next 2 days it increased its forward speed slightly; the area of cloudiness and intense convection increased and became quite striking on the satellite picture for the 23d. Subsequently, the wave slowed its forward speed, and the thunderstorm activity diminished. At the same time both the weak confluence and cyclonic curvature, previously noted in the 2,000-ft streamlines, and the surface pressure trough intensified beneath the upper wave (see also fig. 3). A closed vortex formed near 14.5°N prior to 1200 GMT on the 25th, producing 4-mb pressure falls at Dakar and over the Cape Verde Islands. On the 30th, after reaching long. 45°E, it became a tropical storm.

Wave W–3 (later to become hurricane Beulah) appears first on the 22d near the eastern edge of the analysis network (figs. 5–13). A widespread area of enhanced rainfall and convection east of the Cameroon Mountains

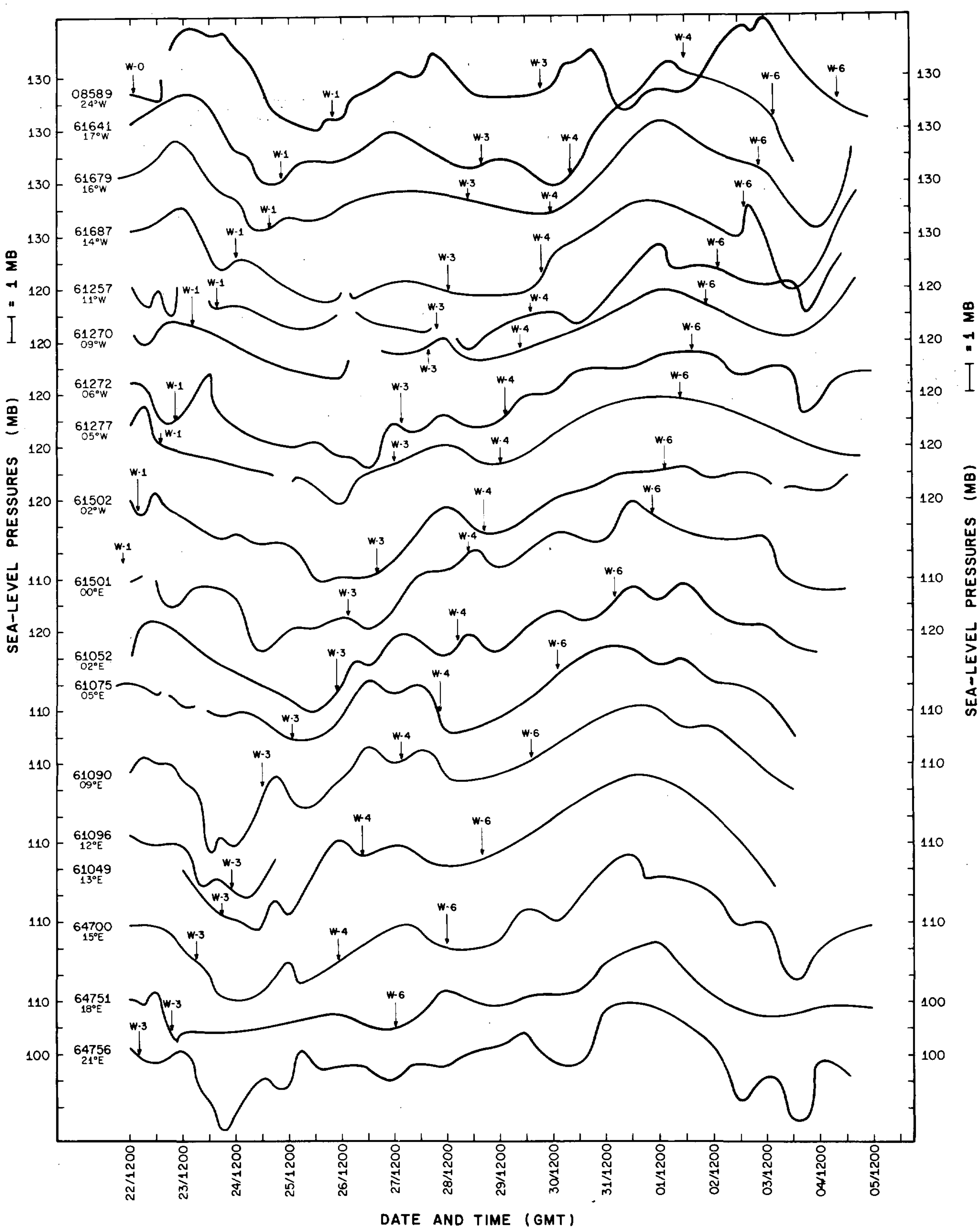


FIGURE 3.—Time variation of diurnally corrected sea-level pressure in millibars for stations situated approximately along lat. 14°N and at the longitude indicated below the station identification number. The approximate mean pressure for each station during the period (in millibars and tenths above 1000) is shown in the margins.

(15°E long.) accompanied the wave's passage westward across these mountains. After its arrival over their west slopes on August 24 the rainfall area became more coherent, while the convection itself was confined to a relatively narrow zone between 10° and 18°N lat. Cyclonic circulation and confluence in the 2,000-ft streamlines became more noticeable after the 27th, and a closed vortex formed beneath the wave axis at 12°N on

332-282 O - 69 - 7

the 29th. Pressure falls associated with the depression amounted to 2 mb at Dakar and the Cape Verde Islands. It remained quiescent, however, for some time, and it was not until September 8 at long. 60°W that the depression became a tropical storm.

Wave W–4 may have formed within the data network and appears first as a weak perturbation near long. 15°E on August 26 (figs. 9–14). It intensified during the following day and subsequently arrived near the coast on August 30, where it closely resembled the preceding two waves. The satellite photograph for the 30th shows a widespread cloud system with cyclonic bands whose center of circulation coincides with a newly formed depression just offshore at lat. 14.5°N. Pressure falls associated with this vortex were about 2 mb (fig. 3) at Dakar and the Cape Verde Islands. The disturbance maintained its circular cloud pattern for a few days, but despite its likely appearance it failed to develop.

Wave W–6 (later to become hurricane Chloe) was first noticed near long. 15°E on the 27th (figs. 10–18) along with some increase in convective activity east of the Cameroon Mountains. It moved westward unaccompanied by any appreciable cloudiness or convection until September 3, when numerous thunderstorms appeared some distance behind the wave axis. During the next 2 days the increase in low-level circulation and precipitation was rather dramatic, and on September 3 a vortex began to form overland southeast of Dakar. The circulation, whose circular banding and definite center are strikingly apparent on the satellite picture for September 4, coincided with a depression located at 14.5°N. Pressure falls of 4 mb were observed along the African coast and over the Cape Verde Islands (fig. 3) as the system passed westward. On September 8 at long. 38°W it achieved the status of a tropical storm.

## 5. DISCUSSION

Figures 4–18 (a–c) illustrate some of the details associated with the passage of traveling wave disturbances across West Africa and the extreme eastern tropical Atlantic Ocean. The waves moved in a coherent fashion across much of West Africa, and their eastward speed varied from 12 to 20 kt. Far inland, the disturbances were rather difficult to track in the surface pressure field or the 2,000-ft streamlines, even with the aid of satellite pictures. At this stage the magnitude of the surface pressure falls accompanying the disturbances usually did not exceed more than 1 or 2 mb, although the flow pattern often showed weak cyclonic curvature beneath the upper wave. The most positive means for tracking the disturbances over the continent proved to be the 700-mb wind field, although a combination of surface isobars, satellite pictures, and 2,000-ft winds was most helpful in augmenting and supporting the upper air data.

When the waves reached the coast, intensification in the low-level circulation resulted in the development of a depression near or just inland from the coast. At this point the cloud pattern in its vicinity became noticeably circular or banded and was accompanied by a 2- to 4-mb anomaly in central pressure of the vortex. The incipient depression was recognizable during its intensification into a closed vortex by a pronounced shift in the surface winds from northwest to southwest with the passage of the upper wave.

These cloud and rainfall patterns, recognizably associated with the traveling disturbances, were at first widely scattered east of the Cameroon Mountains; once on the other side there was often little convection accompanying the wave, as a consequence of its passage through a region of less convectional instability. Later, as the wave began to encounter more unstable air whose origin was over the warmer water southwest of Dakar, cloudiness increased, and an intensification of the system took place. Figure 2 shows that the rapid development of the surface depression on September 3 occurred as the wave passed through the region of maximum instability. According to Gray (1967), the removal of the strong shear and the subsequent passage of the tropical depression across the warm water south of 15°N would have favored its continuance or intensification, even though the instability was somewhat smaller over the ocean.

The mean distribution of rainfall and thunderstorm activity with respect to the 700-mb position of the wave axis (fig. 19) shows that (at lat. 14°N) the maximum occurred some distance *ahead* of the trough and a minimum immediately *behind*. A minor maximum is also found behind the trough. Such a distribution may be related to the peculiar wind profile, which, unlike that found with the classical Easterly Wave, requires a low-level convergence ahead of the wave and also at lower middle levels behind it. Somewhat contrary to the findings of Arnold (1966), the mean soundings for this 15-day period show that the wave is cold core only up to 500–600 mb and is warm core above, suggesting that the waves are therefore most intense at that level (fig. 20). The combination of upper level warmth and relatively moist conditions in the wave axis at all levels further suggests that the wave structure is closely controlled by the convection, wherein heat of condensation is released predominantly at high levels while the low-level air is cooled by downdraft evaporation in thunderstorms. On the sounding for Sal a pronounced inversion at low levels is recognizable, which suggests the presence of air aloft whose recent origin had been over the desert and whose effect would be to suppress the convection in this area.

A final consideration is the possible origin of the traveling disturbances. Thompson (1965) has stated that easterly waves and traveling disturbance lines have not been detected over the East African synoptic network, but he concedes that such phenomena do exist over West Africa. This study indicates that the wave disturbances formed somewhere east of 10°–15°E and points toward a favorable source region over the high ground that stretches east-

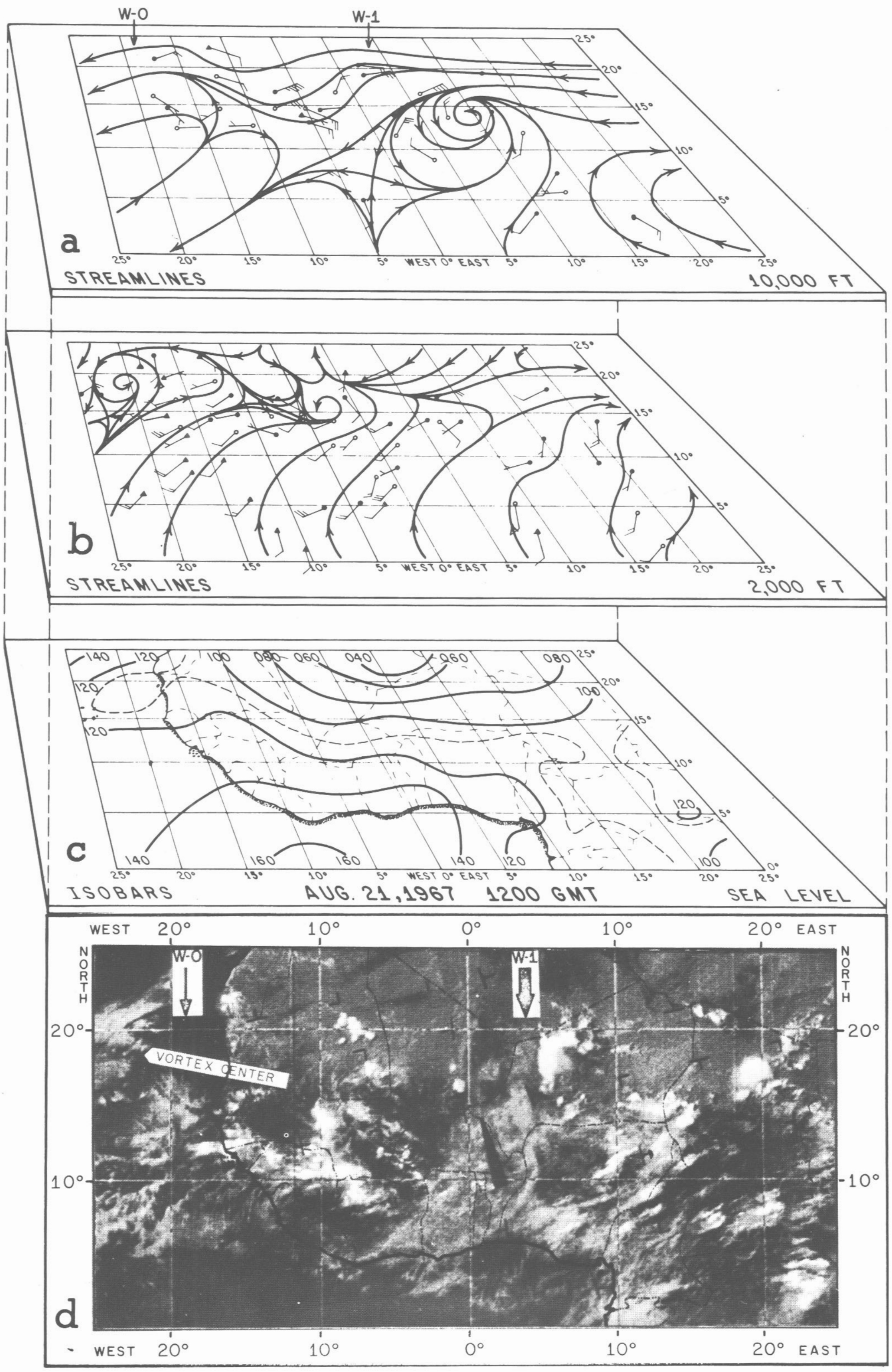


FIGURE 4.—(a) streamlines in perspective at 700 mb for Aug. 21, 1967. The wind vectors at 1200 GMT are plotted at the station location (filled circles). Off-time observations are displaced from their station location according to the wave speed (open circles). Off-level winds, pertaining to the 7,000- or 13,000-ft levels, are signified by a triangle. The longitudinal positions of the upper wave axis are designated by an arrow at the top. (b) same as figure 4a but for 2,000 ft. Off-level wind sectors refer to surface (coastal) or ship reports. (c) surface isobars at 1200 GMT, Aug. 21, 1967. Contour intervals (solid and dashed lines) are labeled in millibars and tenths above 1000. (d) digitalized mosaic of ESSA–5 satellite photograph (Orbits 1560–1561) at approximately 1500 GMT, Aug. 21, 1967. Wave axes are indicated as in figure 4a.

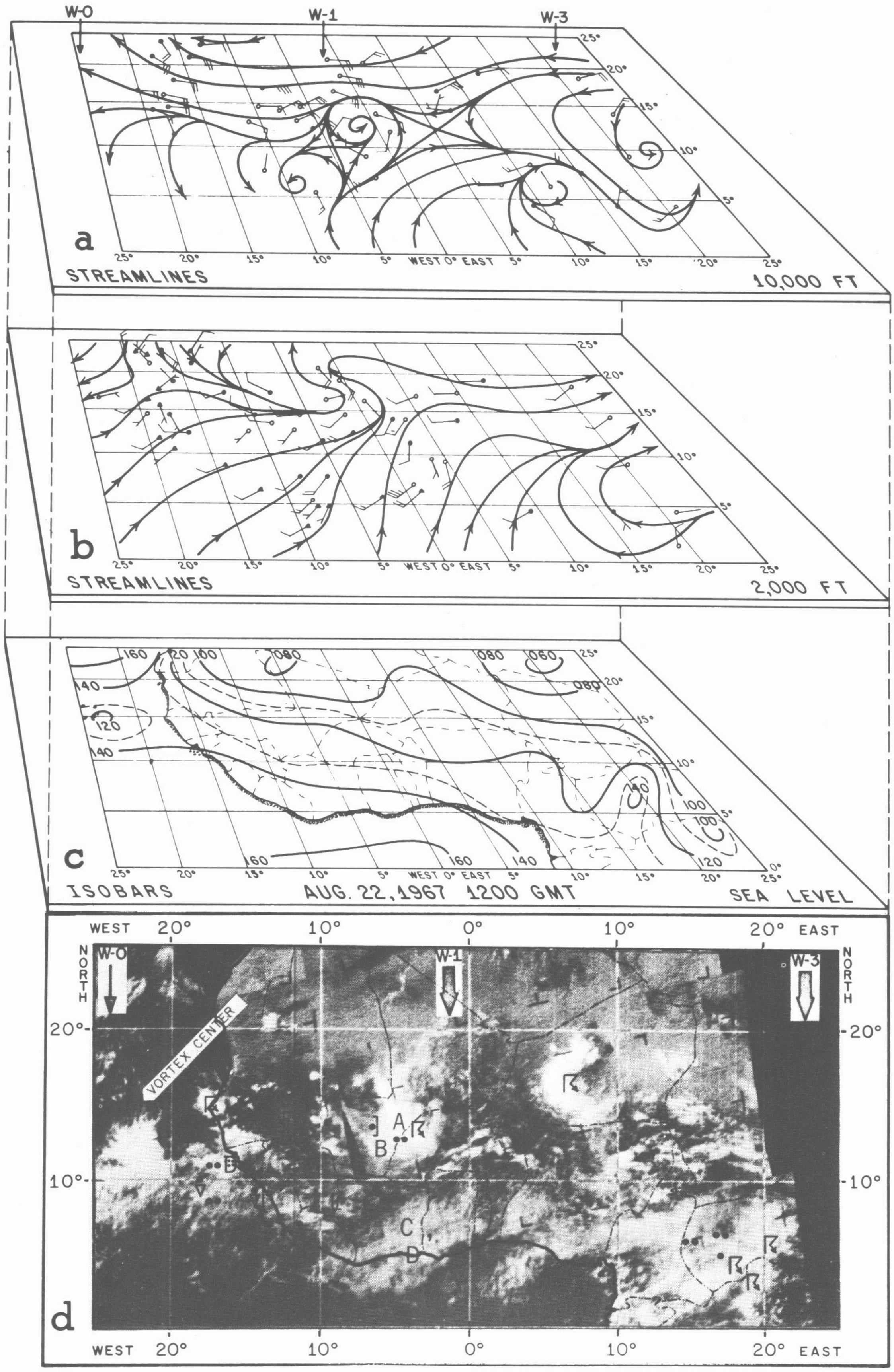


FIGURE 5.—Same as figures 4 (a–d) except for Aug. 22, 1967. On the satellite photograph (Orbits 1573–1574, 1425–1619 GMT), the letters A (intense convection), B (weak convection), C (stratiform), D (rain without thunderstorms), E (broken), and F (fair weather) pertain to the descriptions given in the text. Various weather symbols are also shown.

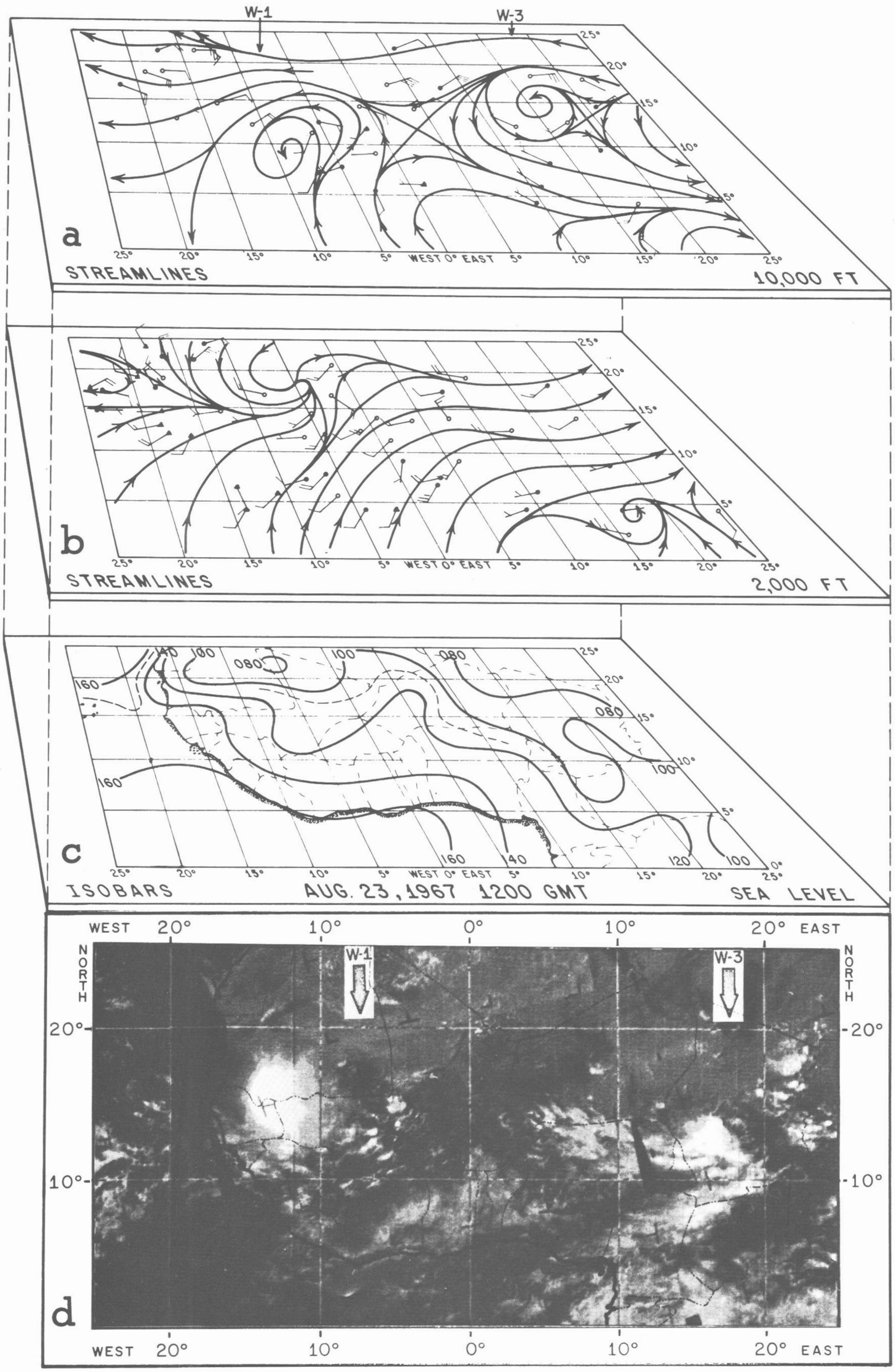


FIGURE 6.—Same as figures 4 (a–d) except for Aug. 23, 1967, Orbits 1585–1587, 1308–1655 GMT.

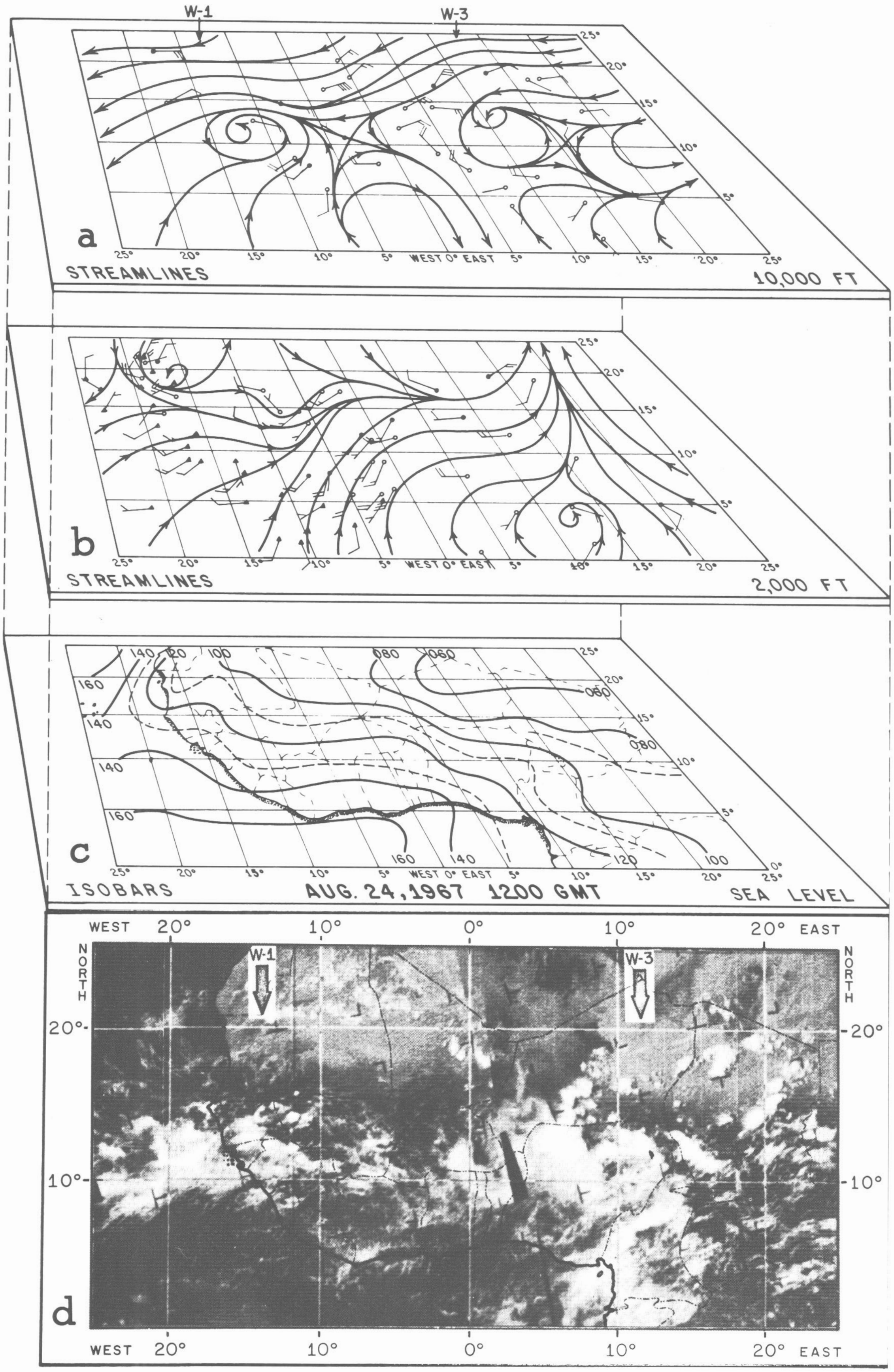


FIGURE 7.—Same as figures 4 (a–d) except for Aug. 24, 1967, Orbits 1598–1599, 1345–1538 GMT.

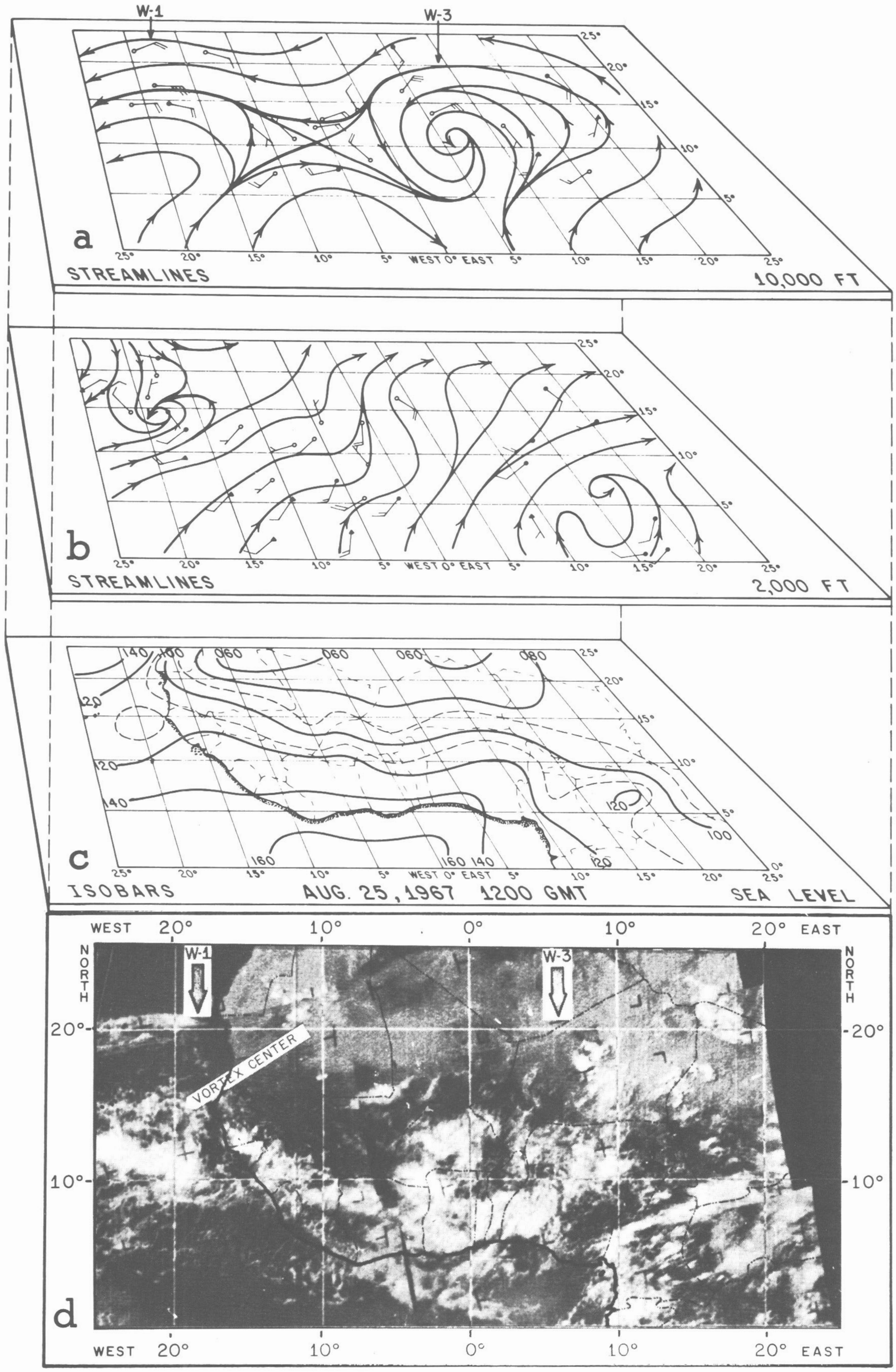


FIGURE 8.—Same as figures 4 (a–d) except for Aug. 25, 1967, Orbits 1611–1612, 1422–1615 GMT.

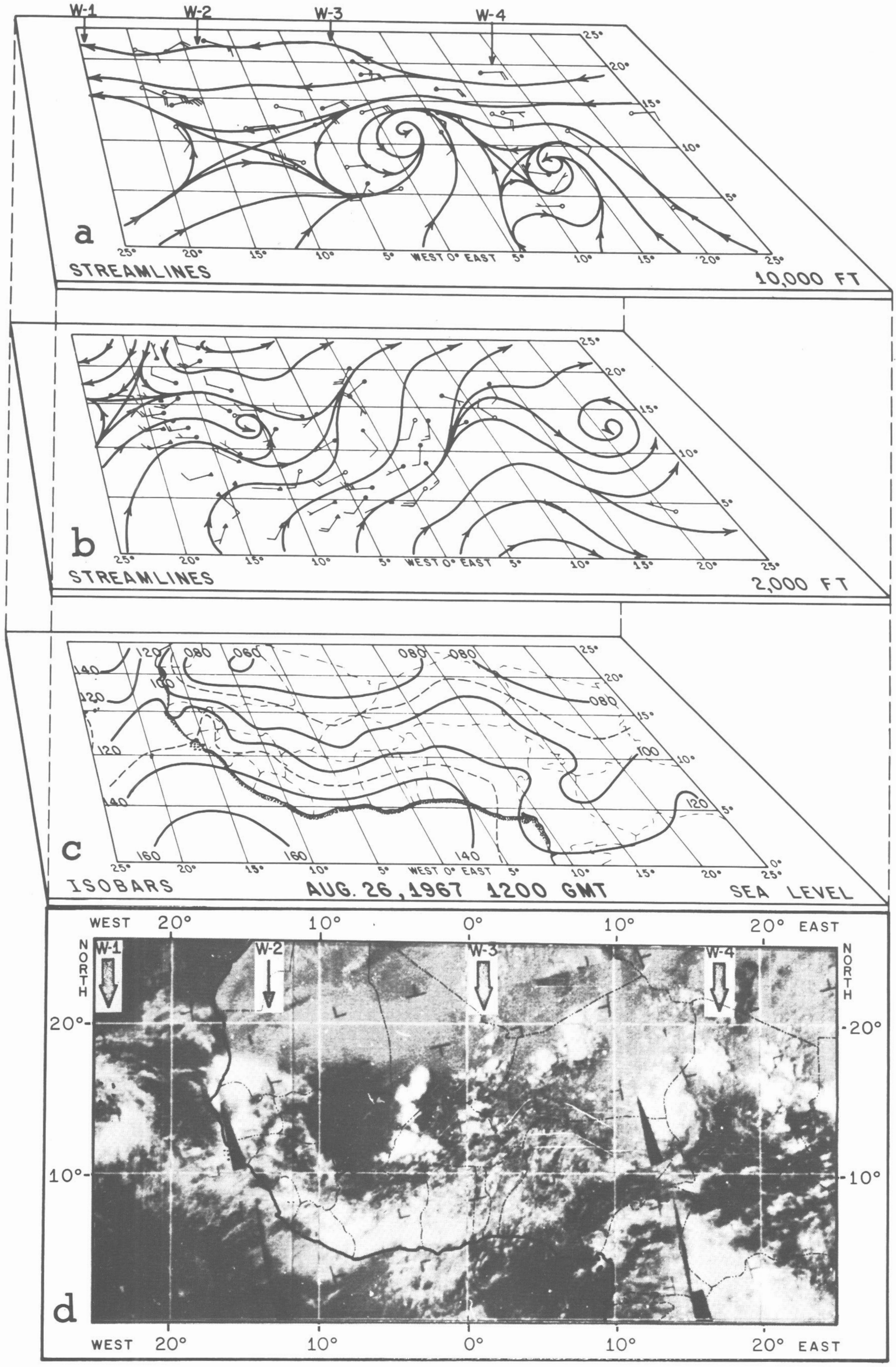


FIGURE 9.—Same as figures 4 (a–d) except for Aug. 26, 1967, Orbits 1623–1625, 1305–1652 GMT.

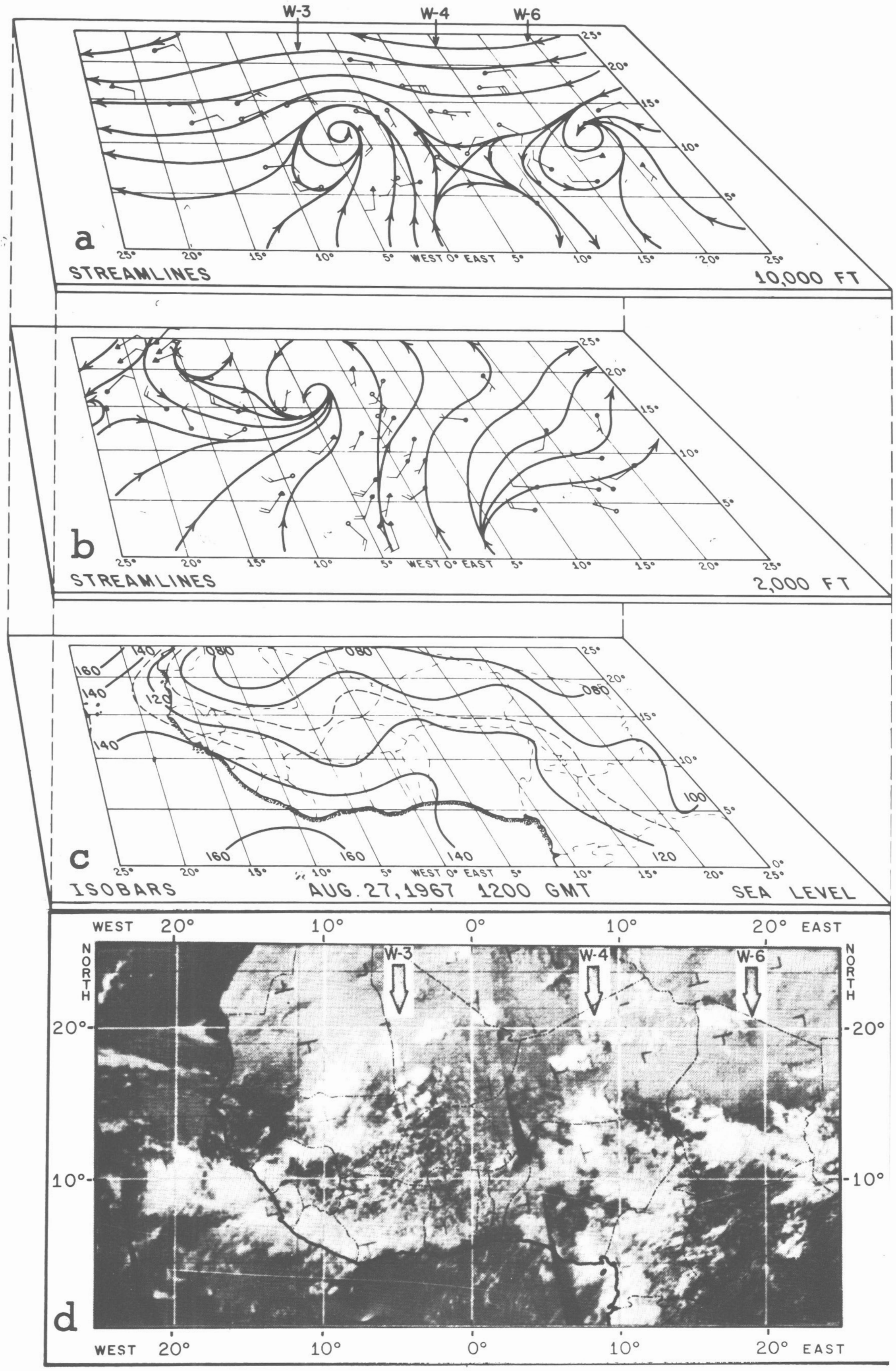


FIGURE 10.—Same as figures 4 (a–d) except for Aug. 27, 1967, Orbits 1636–1637, 1400–1600 GMT.

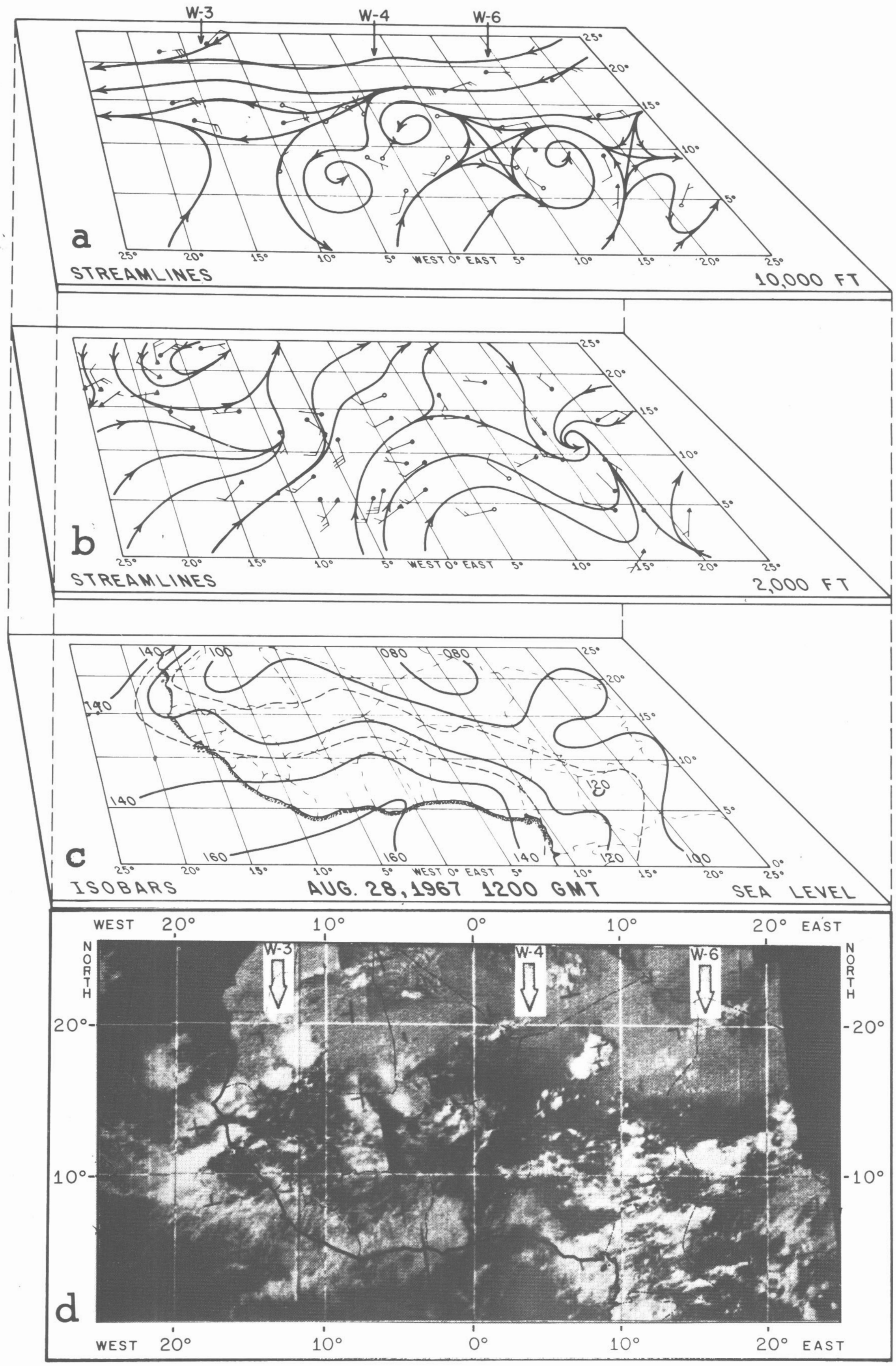


FIGURE 11.—Same as figures 4 (a–d) except for Aug. 28, 1967, Orbits 1649–1650, 1419–1612 GMT.

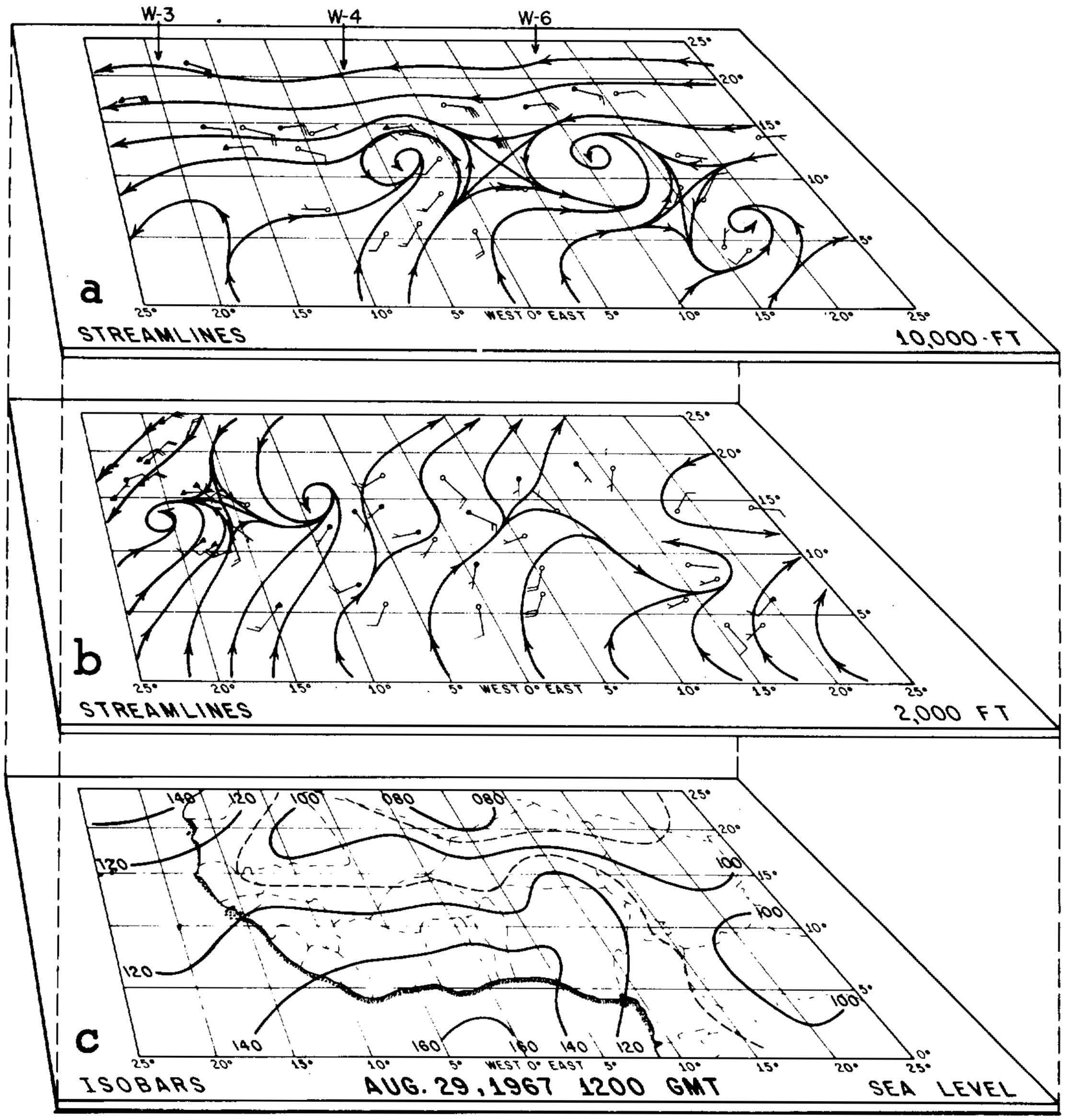


FIGURE 12.—Same as figures 4 (a–c) except for Aug. 29, 1967. (The satellite photograph was voided by transmission difficulty.)

ward from the Cameroon Mountains (Eldridge, 1957, p. 306).

## 6. CONCLUSION

Hurricanes Arlene, Beulah, and Chloe of the 1967 season developed from traveling wave disturbances that were tracked back to the interior of the African Continent. Typically, the disturbances moved westward with little development aloft or reflection at the surface until they approached the western part of the African bulge. There they encountered a supply of highly unstable air at low levels that accommodated a development of the wave into a more intense disturbance and was accompanied by enhanced convection and a formation of a weak depression at the surface. Upon reaching the coast, the convection diminished and became somewhat suppressed, although the area cloudiness and rainfall remained large. While recent evidence suggests that hurricanes and tropical storms not uncommonly originate from African disturbances, the vast majority of such disturbances, including many that are highly similar to or even stronger than these three disturbances, fail to continue their intensification out over the ocean. An example of this is also shown in the analyses.

## ACKNOWLEDGMENTS

I would like to thank Mr. Neil Frank for making available the satellite photographs and for his helpful suggestions along the way. Special credit should go to Mr. Robert Carrodus who was responsible for the imaginative use of perspective in drafting the figures. Additional helpful criticism and comments concerning the manuscript itself were made by Messrs. Neil Frank, Harry Hawkins, and Dr. Banner I. Miller. Mr. Leslie Thomas did the typing.

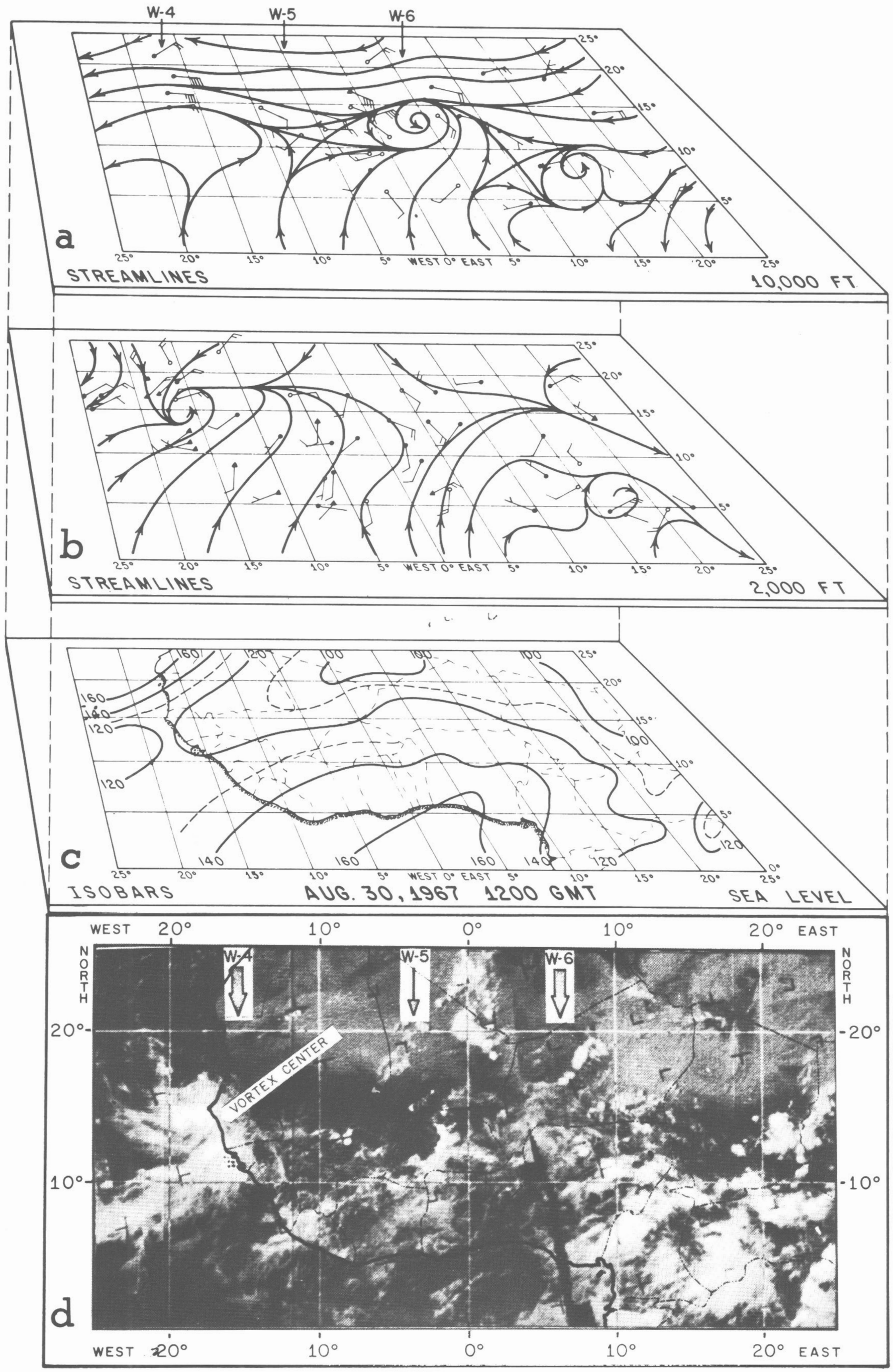


FIGURE 13.—Same as figures 4 (a–d) except for Aug. 30, 1967, Orbits 1674–1676, 1339–1726 GMT.

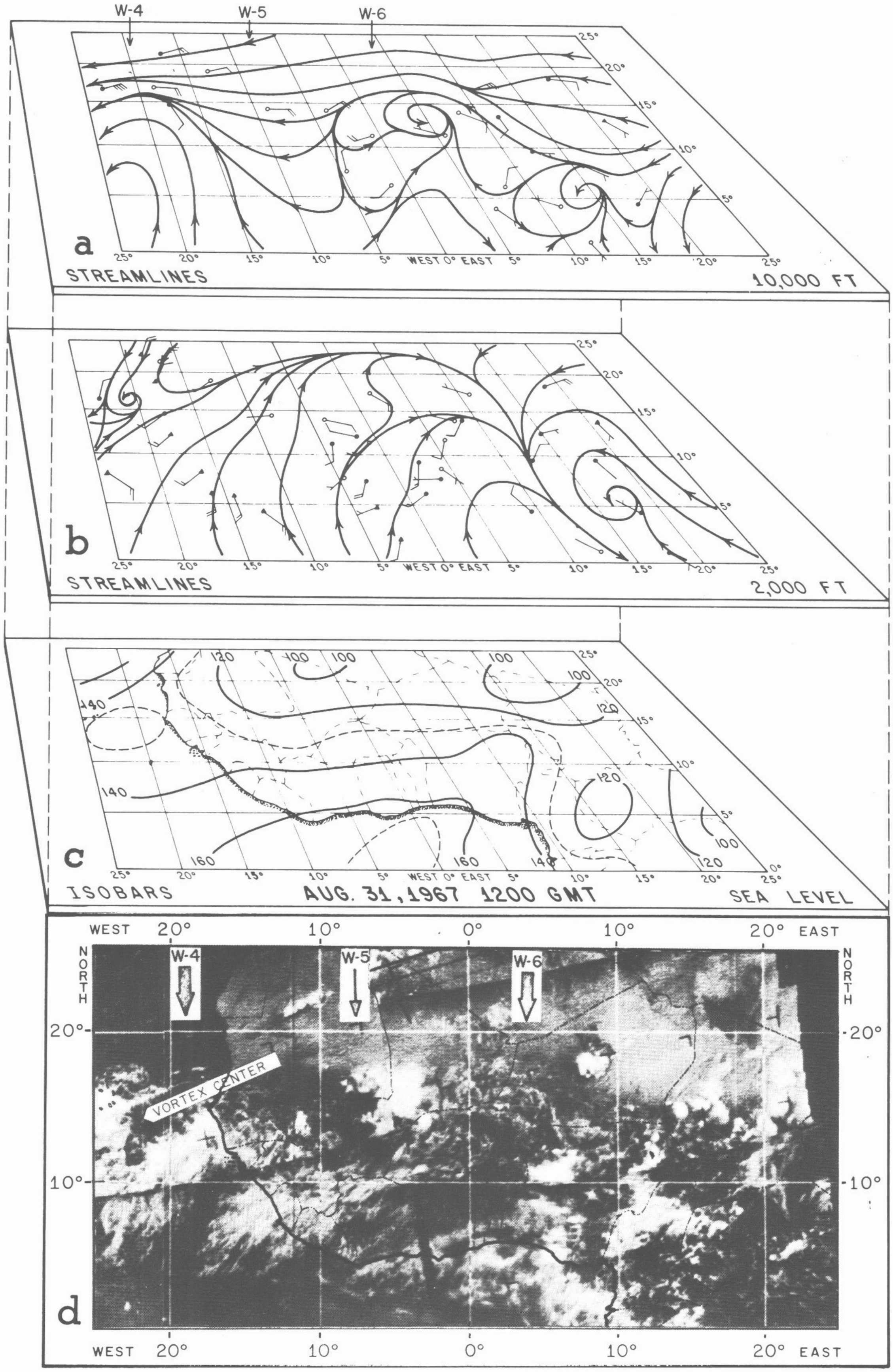


**Figure 14.**—Same as figures 4 (a–d) except Aug. 31, 1967, Orbits 1687–1688, 1415–1609 GMT.

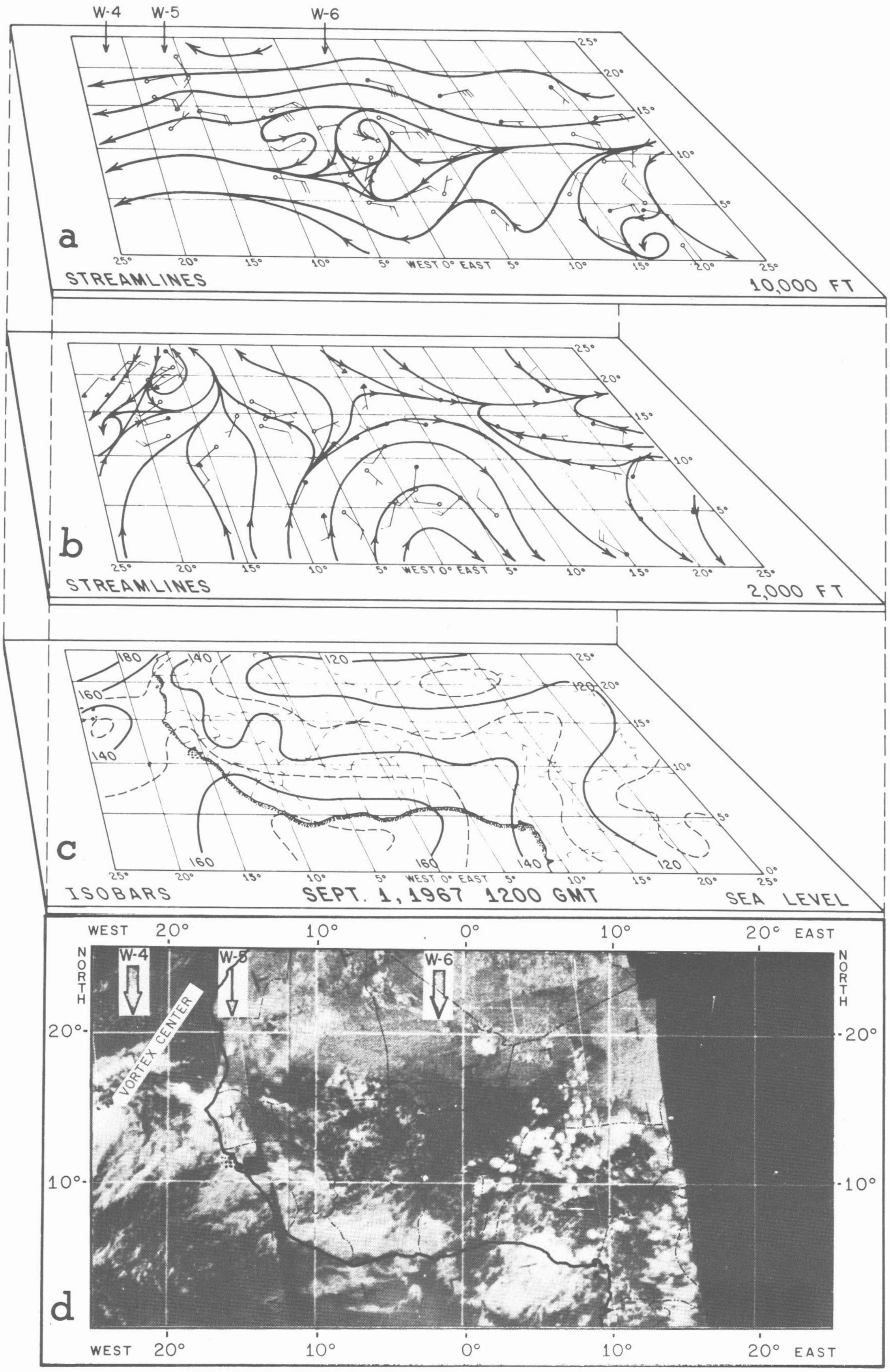


FIGURE 15.—Same as figures 4 (a–d) except for Sept. 1, 1967, Orbits 1700–1701, 1452–1645 GMT.

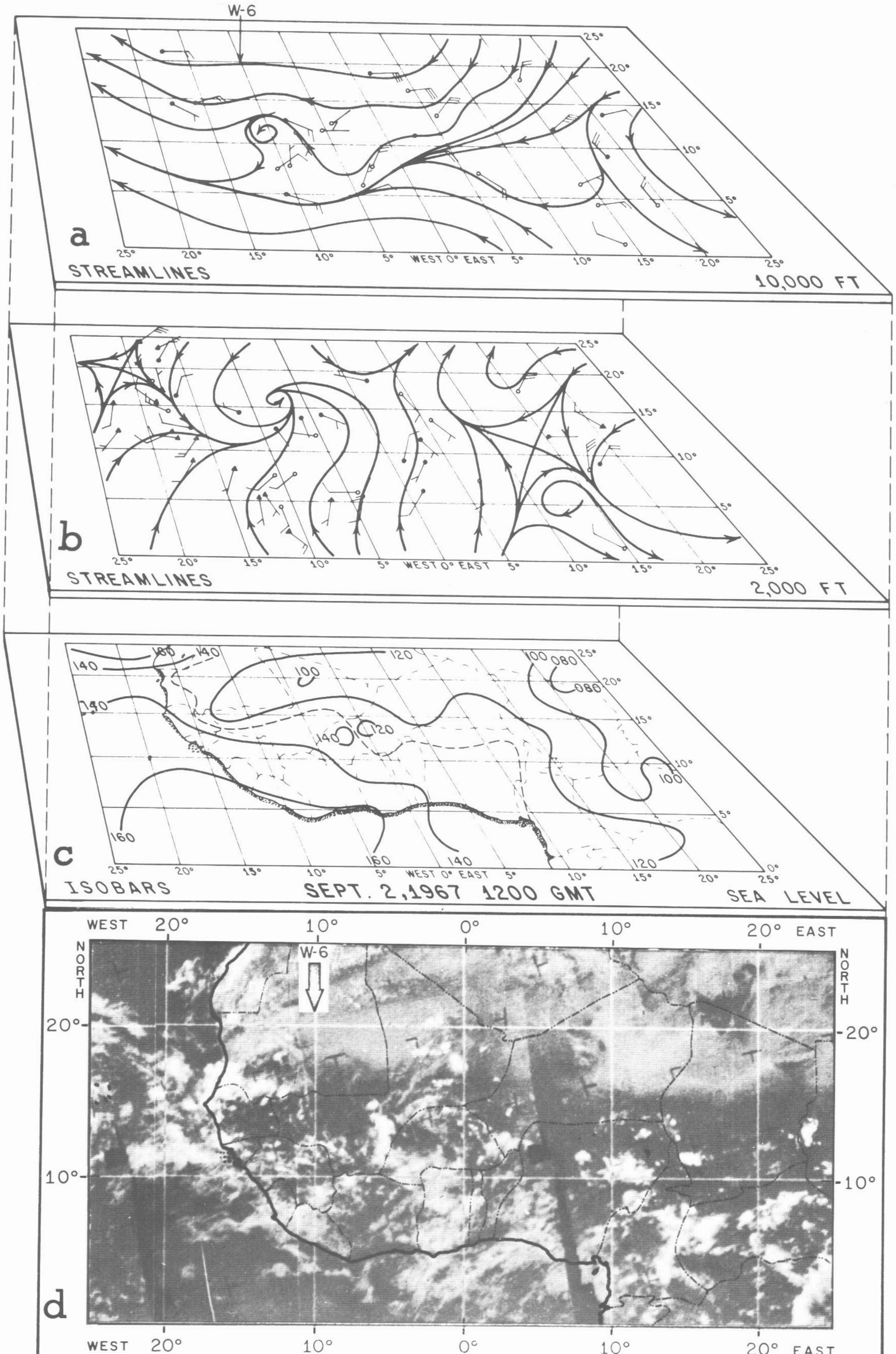


FIGURE 16.—Same as figures 4 (a–d) except for Sept. 2, 1967, Orbits 1712–1714, 1335–1722 GMT.

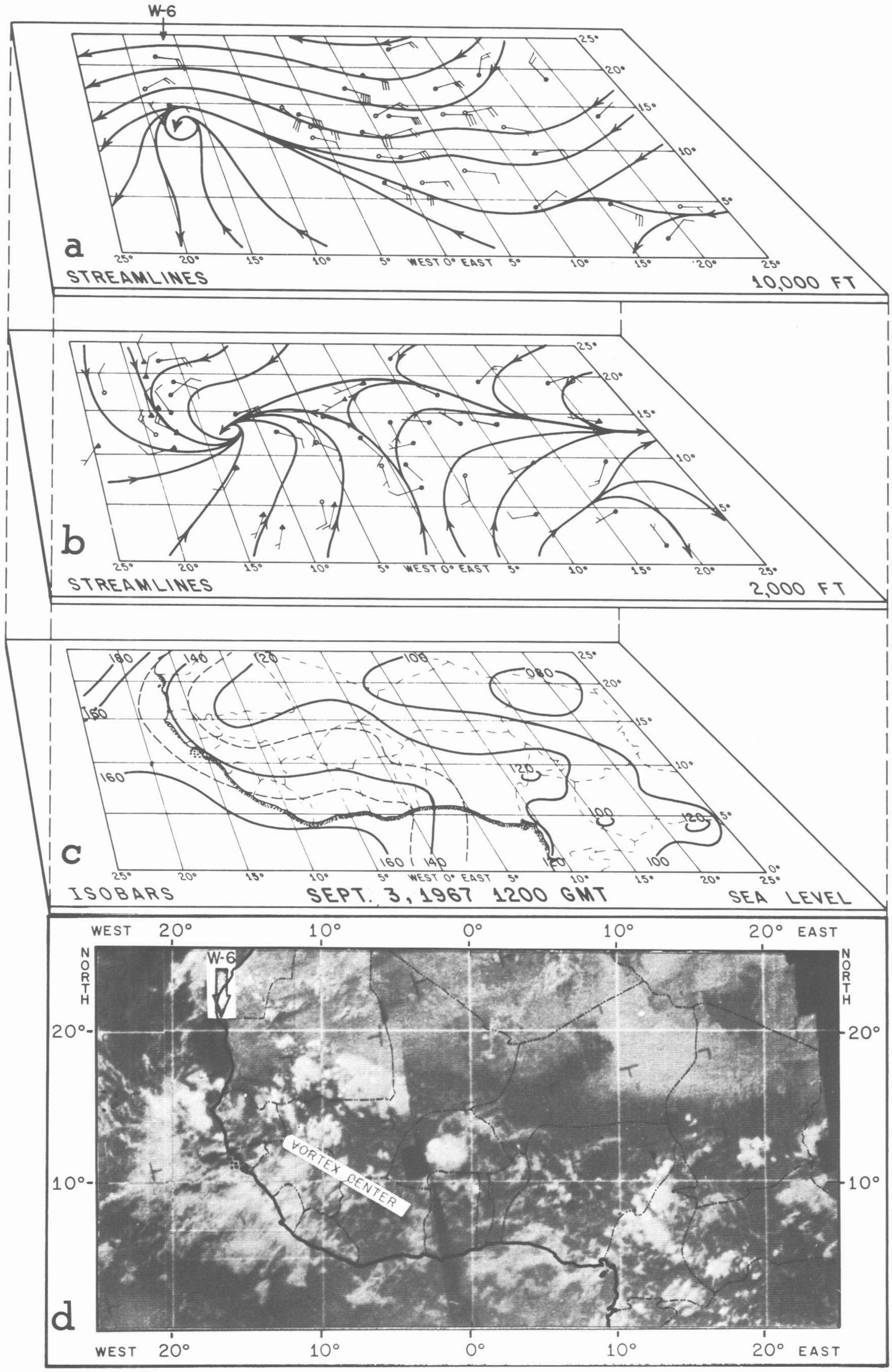


**Figure 17.**—Same as figures 4 (a–d) except for Sept. 3, 1967, Orbits 1725–1726, 1412–1605 GMT.

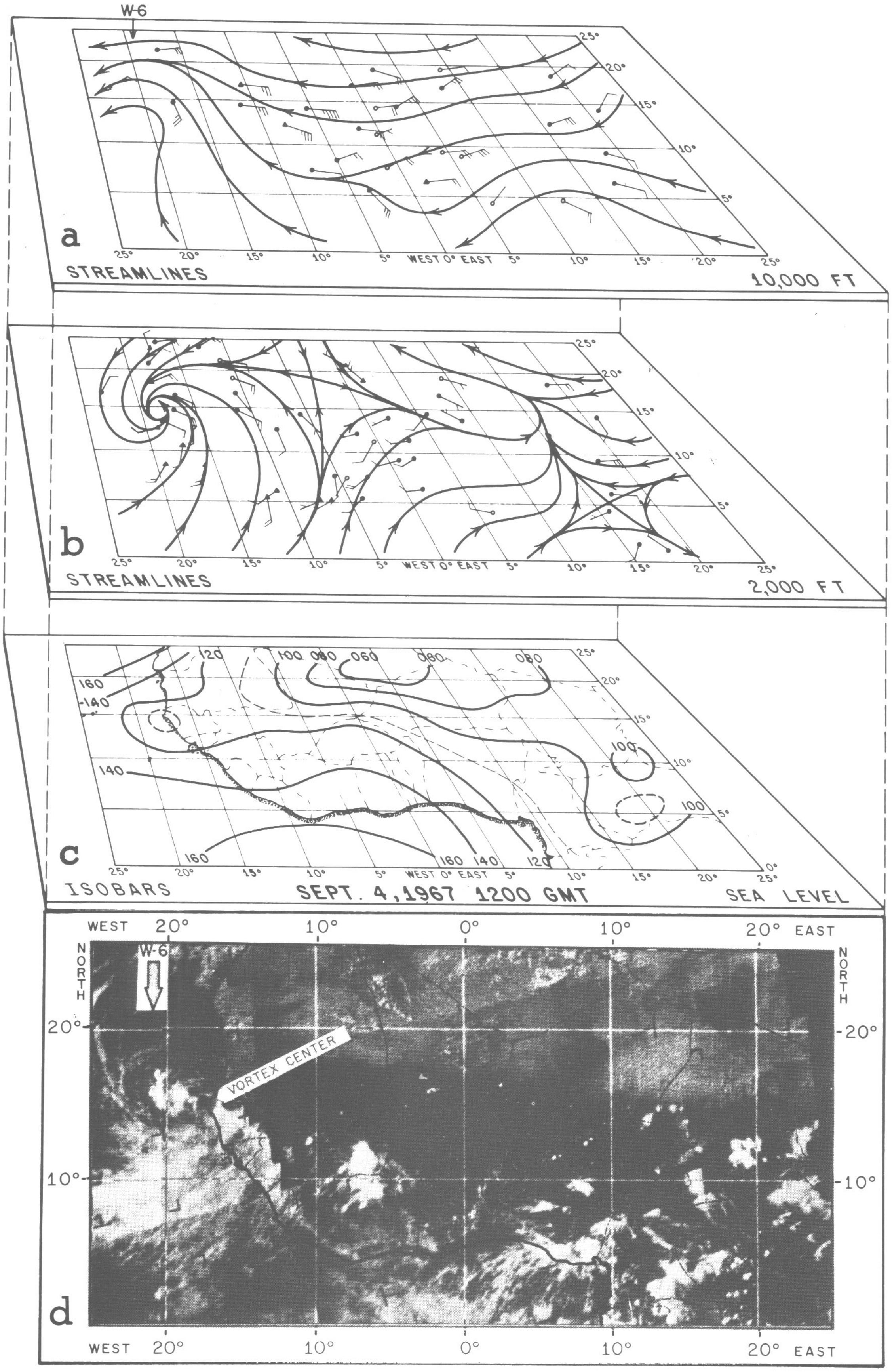


FIGURE 18.—Same as figures 4 (a–d) except for Sept. 4, 1967, Orbits 1738–1739, 1335–1642 GMT.

## REFERENCES


Arnold, J. E., "Easterly Wave Activity over Africa and in the Atlantic with a Note on the Intertropical Convergence Zone During Early July 1961," *Satellite and Mesometeorology Research Project Research Paper* No. 65, Department of Geophysical Sciences, University of Chicago, Dec. **1966,** 23 pp.


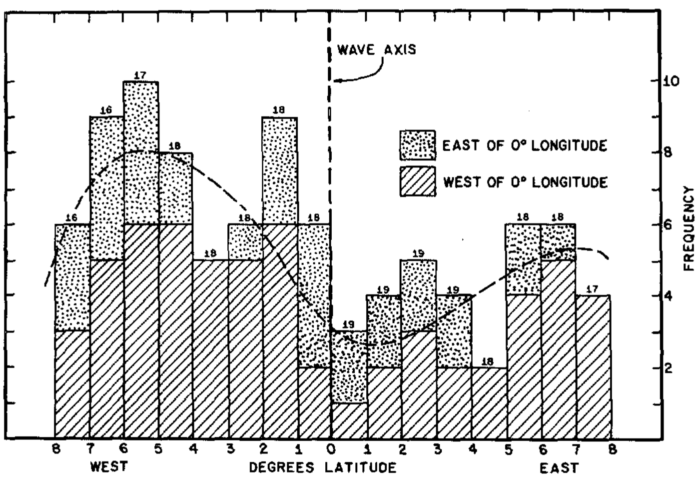


FIGURE 19.—Frequency distribution of disturbed weather (weather categories A, B, or D—see text) per degree of longitude versus distance from the wave axis for waves W–1, W–3, W–4, and W–6. Shaded and open bars refer to waves situated west and east of long. 0°, respectively. The figure at the top of the bar refers to the number of observations for that interval.


Dunn, G. E., "The Hurricane Season of 1960," *Monthly Weather Review,* Vol. 89, No. 3, Mar. **1961,** pp. 99–108.

Dunn, G. E., and Staff, "The Hurricane Season of 1961," *Monthly Weather Review,* Vol. 90. No. 3, Mar. **1962,** pp. 107–119.

Dunn, G. E., and Staff,"The Hurricane Season of 1962," *Monthly Weather Review,* Vol. 91, No. 4, Apr. **1963,** pp. 199–207.

Dunn, G. E., and Staff, "The Hurricane Season of 1964," *Monthly Weather Review,* Vol. 93, No. 3, Mar. **1965,** pp. 175–187.

Eldridge, R. H., "A Synoptic Study of West African Disturbance Lines," *Quarterly Journal of the Royal Meteorological Society,* Vol. 83, No. 357, July **1957,** pp. 303–314.

Erickson, C. O., "An Incipient Hurricane Near the West African Coast," *Monthly Weather Review,* Vol. 91, No. 2, Feb. **1963,** pp. 61–68.

Gray, W. M., "Global View of the Origin of Tropical Disturbances and Storms," *Atmospheric Science Paper* No. 114, Colorado State University, Fort Collins, Oct. **1967,** 105 pp.

Reiter, E. R., *Jet-Stream Meteorology,* University of Chicago Press, **1963,** 515 pp.

Simpson, R. H., Frank, N., Shideler, D., and Johnson, H. M., "Atlantic Tropical Disturbances, 1967," *Monthly Weather Review,* Vol. 96, No. 4, Apr. **1968,** pp. 251–259.

Sugg, A. L., "The Hurricane Season of 1965," *Monthly Weather Review,* Vol. 94, No. 3, Mar. **1966,** pp. 183–191.

Sugg, A. L., "The Hurricane Season of 1966," *Monthly Weather Review,* Vol. 95, No. 3, Mar. **1967,** 131–142.

Thompson, B. W., *The Climate of Africa,* Oxford Press, New York, **1965,** 132 pp.


[*Received July 22, 1968; revised September 9, 1968*]

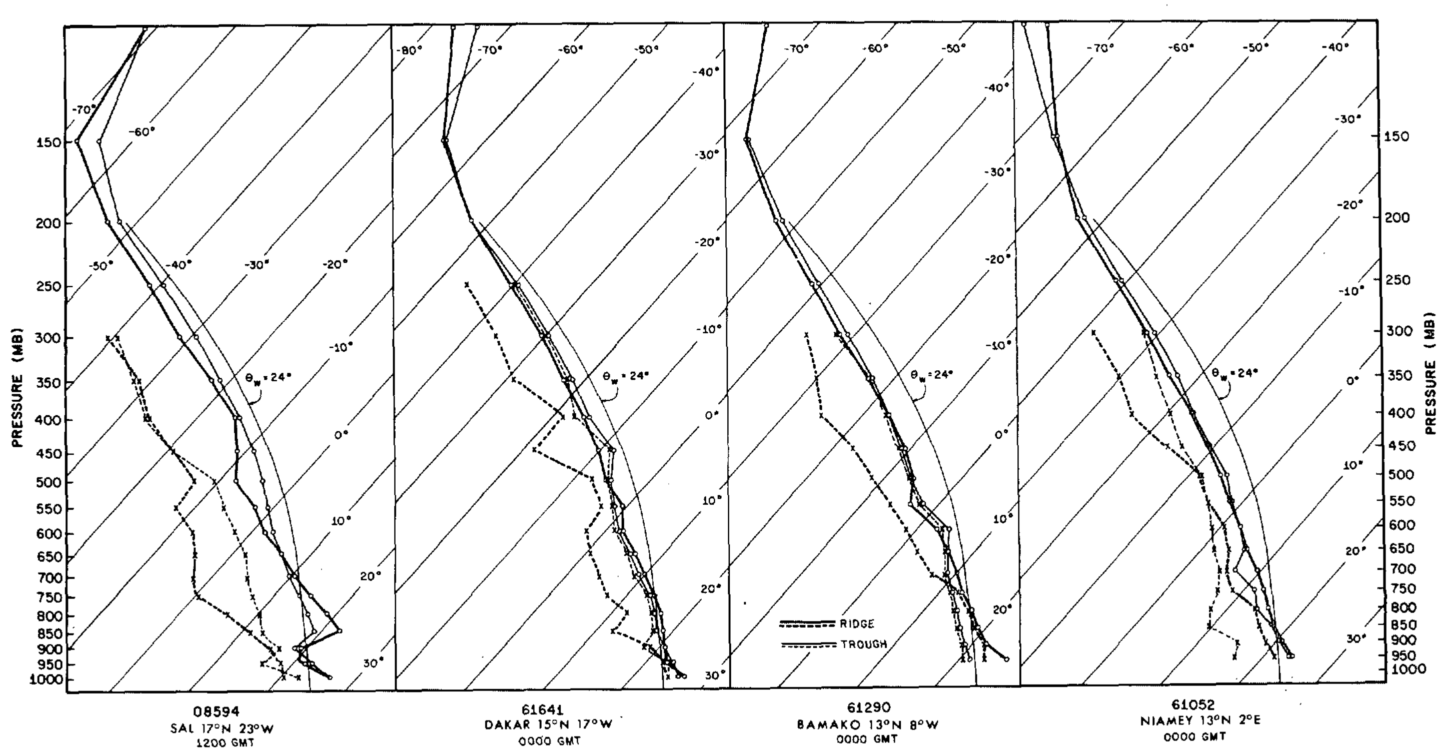


FIGURE 20.—Skew-T diagram for four West African radiosonde stations. Each sounding represents an average of about three individual ones that were made when the station was either close to the axis of one of the four major waves (light solid and dashed curves for temperature and dewpoint respectively) or near the ridge lines on either side of the trough (heavy solid and dashed curves). Temperature and pressure coordinates are labeled in °C and millibars. The wet-bulb potential temperature curve, $\theta_w = 24°C$, is also drawn.